THE ANNALS OF "DUNAREA DE JOS" UNIVERSITY OF GALATI.
FASCICLE IX. METALLURGY AND MATERIALS SCIENCE
N^0. 3 – 2013, ISSN 1453 – 083X

PHOTOCATALYTICAL ACTIVITIES OF MANGANESE DOPED ZINC OXIDE NANOPARTICLES PREPARED BY SOL-GEL METHOD

Mariana (BUŞILĂ) IBĂNESCU[1], *Viorica MUŞAT[1], Torsten TEXTOR[2], Boris MAHLTIG[3]

[1]Centre of Nanostructures and Functional Materials-CNMF, "Dunărea de Jos" University of Galaţi, 111, Domnească Street, 800201, Galaţi, Romania
[2]DeutschesTextilforschungszentrum Nord-West GmbH, DTNW GmbH, Adlerstr. 1, 47798 Krefeld, Germany and CENIDE, Center for Nanointegration Duisburg-Essen
[3]University of Applied Sciences, Faculty of Textile and Clothing Technology, Webschulstr, 31, 41065 Mönchengladbach, Germany
*Corresponding author: viorica.musat@ugal.ro.

ABSTRACT

In the last period, ZnO and doped ZnO nanoparticles are intensively investigated for their photocatalytic properties. This paper reports on ZnO and Mn-doped ZnO nanoparticles obtained by modified sol-gel method. Were studied the structural and optical properties by using x-ray diffraction (XRD) data and visible absorbtion spactra.

The photocatalytic activity of nanoparticles was investigated based on the degradation of the Methylene Blue (MB) dye solution. The results showed that Mn doping enhanced the photocatalytic activity of ZnO nanoparticles.

KEYWORDS: ZnO nanoparticles, Mn doping, band gap, photocatalysis

1. Introduction

Since the decomposition of water into hydrogen and oxygen on titanium electrode by Fujishima and Honda in 1972, photocatalysis has been established as an efficient process for the mineralization of toxic organic compounds, hazardous inorganic constituents [1] and bacteria disinfection [2] owing to the strong oxidizing agent, i.e., hydroxyl radical (OH•) [3]. Most of these semiconductor photocatalysts have band gap in the ultraviolet (UV) region, i.e., equivalent to or larger than 3.2eV (λ = 387nm). Therefore, they promote photocatalysis upon illumination with UV radiation. Unfortunately solar spectrum consists only of 5–7% of UV light, while 46% and 47% of the spectrum has visible light and infrared radiation, respectively [4]. This minimal extent of UV light in the solar spectrum has particularly ruled out the use of natural source of light for photocatalytic decomposition of organic and inorganic contaminants and bacteria disinfection from water and air on large scale. Surface and volumetric charge recombination is an additional obstacle that hinders heterogeneous photocatalysis to be an efficient purification method [5]. ZnO has emerged to be a more efficient catalyst as far as water detoxification is concerned because it generates H_2O_2 more efficiently [6], it has high reaction and mineralization rates [7]. Also it has more numbers of active sites with high surface reactivity [8]. ZnO has been demonstrated as an improved photocatalyst as compared to commercialized TiO_2 based on the larger initial rates of activities [9] and its absorption efficacy of solar radiations [10]. However, ZnO has almost the same band gap (3.2eV) as TiO_2. Surface area and surface defects play an important role in the photocatalytic activities of metal oxide. The reason is that, doping of metal oxide with metal and/or transition metals increases the surface defects [11]. In addition it affects the optical and electronic properties [12] and can presumably shift the optical absorption towards the visible region. To improve the photocatalytic activities was doped ZnO with manganese ion (Mn^{2+}) and were carried out studies on photocatalytic activities of Mn-doped ZnO using only UV light as source of radiation and methylene blue as test contaminant. The preliminary results presented in this work show much promise and suggest the need to further explore heterogeneous photocatalysis.

2. Experimental details

2.1 Preparation of undoped ZnO and Mn-doped ZnO (Mn^{2+}:ZnO)

The preparation procedure was basically similar to that of Spanhel [13]. The procedure consists of two major steps. Firstly the suspension of the precursor and secondly the hydrolysis of the precursor to form the zinc oxide nanoparticles. Zinc acetate dihydrate $(ZnAc)_2 \cdot 2H_2O$ (99%-Sigma Aldrich), manganese (II) sulfate monohydrate ($MnSO4 \cdot xH_2O$-0.1; 5; 15 at%,) (99%-Sigma Aldrich, and isopropanol (99,8%-Fluka), were used to prepare the precursor before lithium hydroxide (LiOH-Merk) was used to hydrolyze the precursor.

For synthesizing the catalyst, ~~0,035M of~~ $(ZnAc)_2 \cdot 2H_2O$ in 500 ml 2-propanol was mixed with different concentrations of manganese (II) sulfate by reflux heating 82°C (boiling point) for three hours. Lithium hydroxide dissolved in isopropanol at room temperature was used for nanoparticle precipitation. The ZnO sol was stored at ≤ 4ºC for 24 hours.

For separating Mn-doped ZnO nanoparticles, high-speed centrifugation 4000 rpm/20min was used, followed by several washes and drying.

2.2 Characterization of Nanoparticles

The crystal structures of the product were identified by X-ray diffraction patterns DRON-3 diffractometer system (Burevestnik, USSR) with CoKα radiation, λ= 1.789 Å.

The crystallite size of the particles was calculated with Debye-Scherrer formula:

$$D = \frac{0.94 \cdot \lambda}{\beta \cos\theta}, \quad (1)$$

The value of interplanar distance (*d*) was calculated with Bragg's equation:

$$2d \sin\theta = n \cdot \lambda \quad (2)$$

and lattice parameters:

$$\frac{1}{d^2} = \frac{4\left(h^2 + h \cdot k + k^2\right)}{3a^2} + \frac{l^2}{c^2} \quad (3)$$

The calculation is based on the measurement of full-width at half-maximum (FWHM) values in the corresponding XRD pattern.

The morphology and the composition of the product were examined by scanning electron microscopy (SEM, type Hitachi S 3400N with tungsten cathode, coated with gold Emitech K500X sputter coater, Oxford X-Max SDD X-ray Energy Dispersive Spectrometer (EDS)

Band gap energy value for ZnO nanoparticles was calculated with formula [14]:

$$E = h \cdot \frac{c}{\lambda} \quad (4)$$

UV/Vis Absorption measurements for that material are being carried out using a Cary 5E UV-VIS-NIR Spectrophotometer, Varian Deutschland GmbH with integrating sphere.

2.3 Photocatalytic measurements

Photocatalytic properties of the samples were investigated by measuring the UV absorption at room temperature using a Cary 5E UV-VIS-NIR Spectrophotometer. The photocatalytic activities of doped and undoped samples were evaluated by measuring photodegradation of Methylene Blue (MB) (20 mg/L added to 40 mL in wather) in presence the 0.1g powder of Mn (0.1, 5, 15wt%):ZnO nanoparticles, in Petri dish, under ultraviolet illumination (>251nm) for 1hour.

3. Results and discussions

Crystalline structure of the prepared nanoparticles was characterized by the XRD (Figure 1). The peaks at 2θ = 37.52°, 40.44°, 42.77° were assigned to (100), (002), (101), of ZnO planes, indicating the wurtzite structure. No characteristic peaks of manganese metal or manganese oxides phases were observed in fig 1, indicating that the samples are single crystalline phase.

Using the Debye-Scherrer equation and the halfwidth of the XRD lines, the average values of crystalline size of the samples were calculated based on the (101) crystal plane.

The crystalline phases and the structural parameters as main crystallite size (D), *a* and *c* lattice parameters obtained by quantitative analysis of the XRD patterns shown in Figure 1 are presented in Table 1.

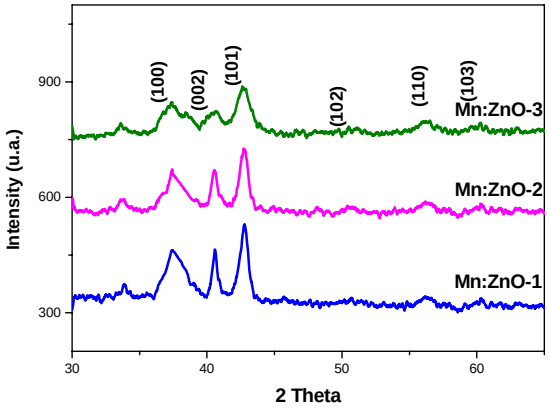

Fig. 1. *XRD patterns for and Mn:ZnO nanoparticles with different concentration: a). Mn:ZnO-1; b) Mn: ZnO-2; c) Mn:ZnO-3*

The crystalline size of photocatalyst decreased with increasing percentage of Mn doping ZnO nanoparticles.

Table 1. *XRD structural parameters for different concentration of Mn doped ZnO nanoparticles*

Sample	Mn	D	*c*	*a*
	[at%]	[nm]	[Å]	
Mn:ZnO-1	0.1	12.9	5,21002	3,24992
Mn:ZnO-2	5	11.8	5,20936	3,25007
Mn:ZnO-3	15	4.2	5,21008	3,25036

For the calculation of the band gap was used optic absorption spectrum. When a semiconductor absorbs photons of energy larger than the gap of the semiconductor, an electron is transferred from the valence band to the conduction band, an abrupt increase in the absorbency of the material occurs to the wavelength corresponding to the band gap energy. The UV-vis optical absorption spectra of as-prepared Mn:ZnO nanoparticles are presented in Fig. 3. The optical absorption edge presents a blueshift to the region of higher photon energy, when Mn concentration increases.

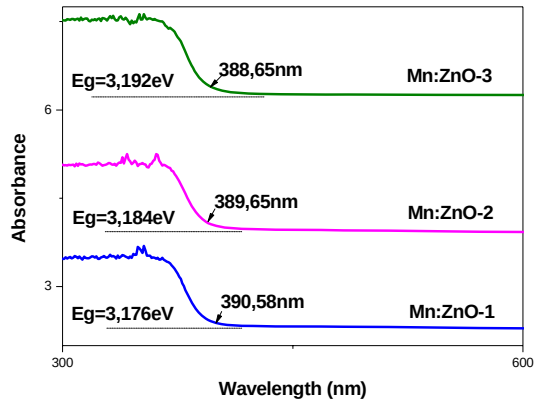

Fig. 3. *UV-VIS Absorption spectra of Mn:ZnO nanoparticles*

These blueshifts confirm preventing the recombination of photoexcited electrons and holes induced by Mn-acceptor doping and so the increase in carrier concentration. The values of optical band gap (Eg) show a widening up to 3.192eV with respect to the values of 3.137eV obtained for ZnO nanoparticles when the Mn – doping concentration increases up to 15at%. In general, according to Burstein–Moss effect, the blueshift of the absorption onset is associated with the increase of the carrier concentration blocking the lowest states in the conduction band [15]. The photocatalytic properties were studied using different concentration of Mn doped ZnO nanoparticles on degradation of methylen blue (MB). The extent of photocatalytic degradation was determined by the reduction in absorbance of the solution. As a result of the reaction between ZnO nanoparticles (through the reactive oxygen species on its surface) and MB dye, the rate of decolorization was changed as was increased the dopant concentration of ZnO nanoparticles.

UV-vis absorption spectra of the residual blanched solution of methylene blue after 60 min UV-irradiation in normal laboratory environment in presence of Mn (different concentration):ZnO as-prepared nanoparticles are shown in Fig.4.

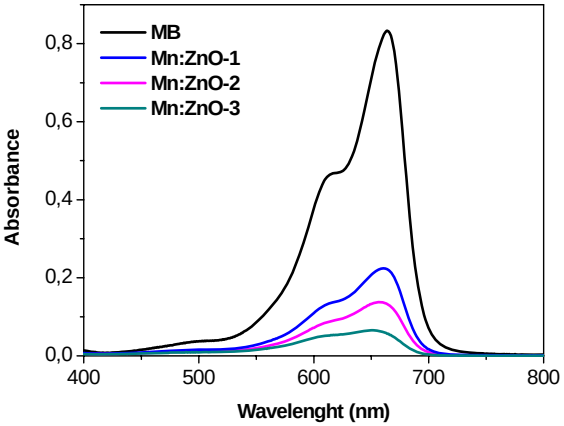

Fig. 4. *UV-Vis absorption spectra of methylen blue in presence by different concentration of Mn doped ZnO nanoparticles (powder) after UV-irradiation, 1h in normal laboratory environment*

Here, was assumed that upon illumination with UV light, Mn:ZnO generates electron–hole pair at the tail states of conduction band and valence band, respectively. The generated electron transfers to the adsorbed MB molecule on the particle surface because it is a cationic dye. The excited electron from the photocatalyst conduction band enters the molecular structure of MB and disrupts its conjugated system which then leads to the complete decomposition of MB. The hole at the valence band generates OH• via reaction with water or OH−, might be used for oxidation of other organic compounds. This clearly demonstrates that ZnO doped with manganese (Mn:ZnO) can be used as a potential photocatalyst, which can operate at visible light and it is evident that doping of ZnO with transition metals like Mn enhances photocatalytic activities of ZnO, and hence Mn:ZnO is capable of degrading MB and other organic dyes even with the UV light irradiation. [16].

4. Conclusions

Mn:ZnO nanoparticles were prepared using a sol-gel process at a temperature below 90°C. Mn:ZnO nanoparticles sol has long stability for further processing.

The XRD measurement confirms that all, Mn-doped ZnO, nanoparticles consist of Wurtzite-type nanocrystallites with different crystalline orientation, (101) being the dominating peak. The Mn atoms substitute Zn sites in the lattice without changing the wurtzite structure. No secondary phases were observed.

The photocatalytic activity of Mn-doped ZnO nanoparticles showed decolorization of a Methylene Blue (MB) solution UV light, as a result of the reaction between the reactive oxygen species from the surface of ZnO nanoparticles and MB dye. The rate of decolorization changed when the Mn:ZnO nanoparticles sample changed. Higher Mn - doping concentration, lower intensity of absorption in visible region, are due to higher photocatalytic activities.

Acknowledgements

The work of Mariana (Busila) Ibanescu was supported by Project SOP HRD – TOP ACADEMIC 78622.

References

[1]. J.M. Herrmann - *Heterogeneous photocatalysis: fundamentals and applications to the removal of various types of aqueous pollutants*, J. Catal. Today 53 (1999) 115–129.

[2]. P.C. Maness, S. Smolinski, D.M. Blake, Z. Huang, E.J. Wolfrum, W.A. Jacoby - *Bactericidal activity of photocatalytic TiO2 reaction: toward an understanding of its killing mechanism*, Appl. Environ. Microbiol. 65 (1999) 4094–4098.

[3]. Z. Huang, P.C. Maness, D. Blake, E.J. Wolfrum, S.L. Smolinski, W.A. Jacoby - *Bactericidal mode of titanium dioxide photocatalysis?* J. Photochem. Photobiol. A 130 (2000) 163–172.

[4]. T. Bak, J. Nowotny, M. Rekas, C.C. Sorrell - *Photo-electrochemical hydrogen generation from water using solar energy*. Materials-related aspects, Int. J. Hydrogen Energy 27 (2002) 1022–27991.

[5]. X.Z. Li, F.B. Li - *Study of Au/Au^{3+}–TiO$_2$ photocatalysts toward visible photo-oxidation for water and wastewater treatment*, J. Enivron. Sci. Technol. 35 (2001) 2381–2387.

[6]. E.R. Carraway, A.J. Hoffman, M. Hoffmann - Environ. Sci. Technol. 28 (1994) 786–793.

[7]. I. Poulios, D. Makri, X. Prohaska - *Photocatalytic treatment of olive milling waste water, oxidation of protocatechuic acid, global nest*, Int. J. 1 (1999) 55–62.

[8]. B. Pall, M. Sharon - *Enhanced photocatalytic activity of highly porous ZnO thin films prepared by sol–gel process*, Mater. Chem. Phys. 76 (2002) 82–87.

[9]. K.Y. Jung, Y.C. Kang, S.B. Park - *Photodegradation of trichloroethylene using nanometre-sized ZnO particles prepared by spray pyrolysis*, J. Mater. Sci. Lett. 16 (1997) 1848–1849.

[10]. S. Sakthivel, B. Neppolian, M.V. Shankar, B. Arabindoo, M. Palanichamy, V. Murugesan - Solar Energy Solar Cells 77 (2003) 65–82.

[11]. R. Wang, J.H. Xin, Y. Yang, H. Liu, L. Xu, J. Hu - *The characteristics and photocatalytic activities of silver-doped ZnO nanocrystallites*, Appl. Surf. Sci. 227 (2004) 312–317.

[12]. K. Vanhesuden, W. L. Warren, J. A. Voigt, C. H. Seager, D.R. Tallant - *Impact of Pb doping on the optical and electronic properties of ZnO powders*, Appl. Phys. Lett. 67 (1995) 1280–1282.

[13]. Spanhel, L., Anderson, M. A. - J. Am. Chem. Soc. 1991, 113, 2826

[14]. *** - Jayant Dharma-PerkinElmer Technical Center; Aniruddha Pisa-Global Application Laboratory PerkinElmer, Inc. Shelton, CT USA, *Simple Method of Measuring the Band Gap Energy Value of TiO2 in the Powder Form using a UV/Vis/NIR Spectrometer.*

[15]. X. Zi-Qiang, D. Hong, L. Yan, C. Hang - *Al-doping effects on structure, electrical and optical properties of c-axis-orientated ZnO:Al thin films*, Materials Science in Semiconductor Processing 9 (2006) 132–135.

[16]. Ullah R., Dutta J. - *Photocatalytic degradation of organic dyes with manganese-doped ZnO nanoparticles,* Journal of Hazardous Materials 156 (2008) 194–200